Engineering Structures 34 (2012) 81–94

Contents lists available at SciVerse ScienceDirect

Engineering Structures

journal homepage: www.elsevier.com/locate/engstruct

Dynamic response control of multi-story structures by isolators with multiple plane sliding surfaces: A parametric study

Muhannad Y. Fakhouri [a,*], Akira Igarashi [b]

[a] Department of Urban Management, Graduate School of Engineering, Nishikyo-ku, Kyoto University, Kyoto 615-8540, Japan
[b] Department of Civil and Earth Resources Engineering, Graduate School of Engineering, Nishikyo-ku, Kyoto University, Kyoto 615-8540, Japan

ARTICLE INFO

Article history:
Received 24 January 2011
Revised 23 August 2011
Accepted 24 August 2011
Available online 4 November 2011

Keywords:
Base isolation
Sliding isolators
Multiple-slider bearing
Fictitious spring method
Friction coefficient

ABSTRACT

Recently, a type of simple and cost effective sliding isolator, namely the uplifting sliding bearing (UPSS), had been developed for ensuring the seismic performance of multi-span continuous bridges. The objective is to control the large horizontal displacement of the conventional rubber bearings using this new sliding device which has a high potential in reducing the horizontal displacement due to the uniqueness of its geometrical configuration. The UPSS device consists of multiple sliding surfaces connected together, based on the PTFE and SUS interface; one horizontal and two inclined surfaces. This paper aims to investigate the efficiency of using the multiple-slider bearing based on the concept of UPSS to isolate multi-story shear type structures. The principles of operation and force displacement relationship for the isolator are introduced. The seismic behavior of the base isolated building by the multiple-slider bearing subjected to seismic excitation is investigated, comparing with conventional rubber bearing and pure friction slider isolating systems. Moreover, extensive parametric investigations are performed in order to achieve an optimum performance of the isolator with respect to three main properties which define the device: clearance length, the inclination angle and the friction coefficient. The results show the effectiveness of the multiple-slider bearing in minimizing the damage from earthquakes. The multiple-slider bearing proves to have a high potential in minimizing the effect of the ground displacement pulses through its operation mechanism and its unique feature that permits the use of different set of friction coefficients on each sliding surface. In addition, a principle to define the optimum value of the friction coefficient is developed.

1. Introduction

Seismic isolation has been proven to be an efficient approach to earthquake resistant-design of structures based on the concept of reducing the seismic demand rather than increasing the seismic resistance capacity of the structure, and is one of the preferable alternatives in seismic retrofitting of historic structures without impairing their architectural characteristics.

In the wake of the Great Hanshin-Awaji Earthquake of 1995 (Kobe, Japan), the effectiveness of seismic isolation structures has been demonstrated and verified. As a result, the number of projects on seismic isolation buildings has been remarkably increased. Seismic isolation has been actively adopted and recognized as a viable technique in construction of bridges, buildings and other structures. Since then, researchers and engineers in this field have been working to develop seismic isolation devices as a part of their efforts to offer earthquake resistant structures and many developed systems have successfully been put forward into practice. Extensive reviews on different types of isolation devices and their applications to structures have been provided by many researches [1–6]. Based on the mechanical characteristics, seismic isolators can be classified as elastomeric or sliding bearings.

Sliding bearings have found more and more applications in recent years over rubber bearing for economic reasons as well as its durability and stability characteristics. Tests of full size sliding bearings show that these isolators retain their full strength and stability throughout their displacement range with high strength factor of safety and with no degradation of hysteretic loop under repeated cyclic loading [7]. The main advantage of sliding isolators over rubber bearings is that the former never resonates to any type of excitation, because sliding mechanisms has no natural period by itself unless extremely strong restoring force overwhelming the friction is applied [8]. Sliding isolators have also been proven to be cost effective and efficient devices on numerous projects to date. In addition, their outstanding performance in cold temperature testing has proven their efficacy in cold weather regions [9]. A considerable amount of theoretical analysis as well as experimental works has been done on isolated structures by pure friction

* Corresponding author. Tel.: +81 80 3136 0490; fax: +81 075 383 3243.
E-mail addresses: m.fakhouri@kt2.ecs.kyoto-u.ac.jp (M.Y. Fakhouri), igarashi.akira.7m@kyoto-u.ac.jp (A. Igarashi).

0141-0296/$ - see front matter © 2011 Elsevier Ltd. All rights reserved.
doi:10.1016/j.engstruct.2011.08.042

isolators (PF) systems subjected to harmonic and earthquake excitations [10–15].

Generally speaking, sliding isolators alone are impractical due to lack of restoring capability. The practical effectiveness of sliding isolators can be enhanced by adding restoring force mechanism to reduce the residual displacements in a level that can be incorporated in structural design requirements. Various sliding isolators including a restoring force mechanism capability have been proposed and studied. Representative examples are: the resilient-friction base isolator (R-FBI) [16], the sliding resilient friction base isolator (SR-F) [17], the TASS system [8], the friction pendulum system (FPS) [18] and the variable frequency pendulum isolator (VFPI) [19].

Recently, a type of isolators with multiple plane sliding surfaces, which is referred to as the uplifting slide bearing [20–23] is developed primarily to be used for upgrading the seismic performance of multi-span continuous bridges. The uplifting slide bearing utilizes a simple sliding mechanism making the use of three PTFE and highly polished stainless steel interface set in series where two of them are made inclined, and is installed on the top of the middle piers and rubber bearings (RB) at the two abutment ends. The main purpose to develop such a device was to fulfill the need for a seismic isolation device that is simple, and effective in reducing the horizontal displacement with a low cost in order to be implemented in multi-span continuous bridges. It was set forward in competence with the laminated rubber bearings which tend to respond with a large horizontal displacement values during earthquake excitations, which in turn leads to a larger expansion joint and an increase in the maintenance cost.

In this study, the efficiency of using isolator with multiple plane sliding surfaces in mitigating the risk of earthquake and preserving multi-story structures, including buildings from damage is investigated. This study also intends to establish the underlying principles of operation in a simplified analytical model through the development of the force–displacement constitutive relationship. In addition, the behavior of isolated multistory buildings using the multiple slider bearing is examined in comparison with the RB and PF isolating systems. Comprehensive parametric studies on the effect of isolator friction coefficients, inclination angle, and the clearance length on the structure response under harmonic excitation are also presented. One of these parametric studies focuses on a unique feature of the multiple-slider bearing which permits the variation of friction coefficient achieved by using different friction coefficient values for each plane sliding surface.

2. Isolator with multiple plane sliding surfaces

The concept and principle of operation of the isolator with multiple plane surfaces is adopted to isolate multi-story structures mainly to control the maximum top floor horizontal displacement. The need for controlling displacement to a minimum level is a vital issue especially in big and crowded cities where building are often built closely to each other because of the limited availability and high cost of the land, possibly causing pounding of adjacent buildings due to the insufficient or inadequate separation and can be a serious hazard in seismically active area [42,43]. Therefore, the geometry of this device was chosen to help in mitigating such a problem by preventing the motion to be fully activated in the horizontal direction, and allowing part of the earthquake transmitted energy to be transferred into a gravitational potential energy through the diagonal sliding. The unique feature of the device mechanism depends essentially on the geometrical configuration of the isolator which consists of one horizontal and two inclined plane sliding surfaces at both ends. These three surfaces based on PTFE slider and stainless steel (SUS) plate interface. During normal or low intensity earthquakes, the isolator behaves as a pure friction isolator with sliding only in horizontal direction. However, during a severe earthquake, sliding will occur on the inclined surface producing displacements in both horizontal and vertical directions, as shown in Fig. 1.

Besides the economical reason and the ease of manufacturing, the hysteretic behavior of this device provides more freedom in the process of design which requires the determination of three parameters: clearance length (L) i.e. the specified distance prior to the diagonal sliding, the inclination angle (θ) and the friction coefficient (μ) for the three surfaces in contact. The configuration of the device as discussed later has the potential of using different frictional bearing in each plane surface which has been found to add more reduction to the horizontal displacement response. It is worth pointing out that the isolator provides an architecturally flexible solution in terms of integration into the structural system for cases in which space consideration is an important factor, rendering the conventional rubber bearing under walls problematic.

3. Simplified mathematical model

In sliding devices, two phases can be assumed as sliding and non-sliding phases. In the non-sliding phase, the shear force at the interface is smaller than the resistance friction force and the structure can be treated as a fixed base system. Once the lateral shear force exceeds the friction force, the structure will start to slide. The horizontal friction force at the sliding interface offers resistance to motion and help in dissipating the energy of structural response.

The free body diagram for the multiple sliding bearing in quasi-static equilibrium can be simplified as shown in Fig. 2. While the horizontal displacement does not exceed L, the structure behaves in the same manner as of a structure isolated by pure friction isolators. Another advantage of the use of the clearance is that it may help in providing a force-soft mechanism that may delay uplift mechanism allowing reduction in restoring force.

The friction force (f_r) in the sliding phase can be expressed by:

$$f_r = \mu N \mathrm{sgn}(\dot{x}_b) \tag{1}$$

where μ is the friction coefficient; N is the normal force; $\dot{x}_b$ is the relative velocity of the bearing slider along the sliding surface, and sgn() is the signum function.

When the displacement exceeds L, the structure starts to slide on the inclined surface. The derivation for the horizontal force (f_h) and its relation with the vertical force (f_v) can be described as:

$$f_h = f_r \cos\theta \pm N \sin\theta \tag{2}$$

$$\frac{f_h}{f_v} = \frac{\pm\mu\cos\theta \pm \sin\theta}{\pm\mu\sin\theta \pm \cos\theta} \tag{3}$$

The sign of each term depends on the direction and the side of motion. The ratio between the horizontal and vertical reaction depends essentially on two important parameters which define the multiple slider bearing i.e. μ and θ. The quasi-static hysteretic behavior can be idealized as shown in Fig. 3.

There are differences in the force–displacement relationship for the case considering dynamic response of the structure and that for the quasi-static equilibrium, including the impact forces generated due to the transition from horizontal to the inclined surfaces, and vice versa [20–23]. However, for simplicity of the analysis, the force–displacement relationship shown in Fig. 3 is regarded as a good approximation that covers the essential characteristics of the device, and is used in the response analysis of the system in this study.

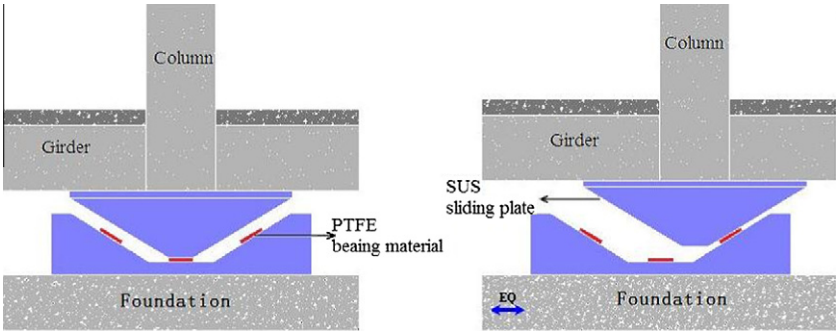

Fig. 1. Schematic diagram of the isolator with multiple plane sliding surfaces.

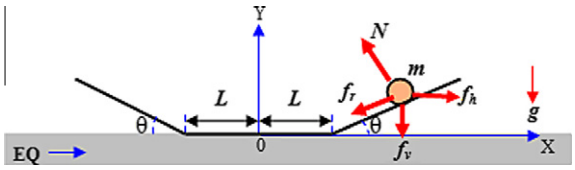

Fig. 2. Mechanical model of the isolator with multiple plane sliding surfaces.

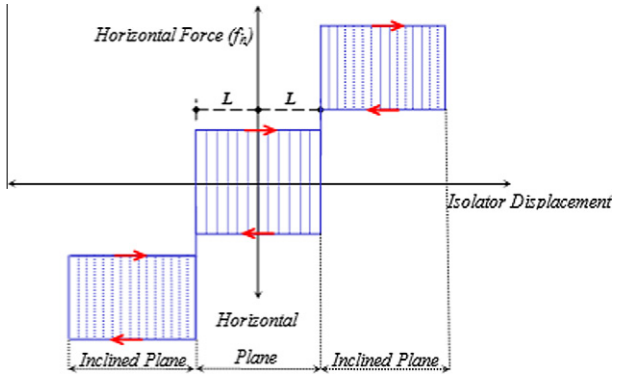

Fig. 3. Idealized force–displacement relationship of multiple-slider bearing for a quasi-static cycle.

4. Coefficient of friction (μ)

One of the most important parameter that controls the dynamic characteristics of sliding isolators is the coefficient of friction. The most popular and well known sliding material is the polytetrafluoroethylene (PTFE) or its DuPont brand name 'Teflon'. It is greatly non-reactive, partly because of the strength of carbon–fluorine bond and it is also a high corrosion resistance material [24]. Due to its low friction of coefficient, with minimum values varies between 0.03 and 0.06 [25], it has been used for several years to accommodate the movement of deck due to thermal variation, creep and shrinkage movement. The friction force which is mobilized at the sliding interface depends on the normal force, bearing pressure, the direction and value of sliding velocity and composition of the sliding interface [26]. Several models have been proposed to model the dynamic friction, including the one expressing the dependency of friction coefficient on the sliding velocity and the bearing pressure by the following expression [27]:

$$\mu = \mu_{\max} - (\mu_{\max} - \mu_{\min})e^{-a|\dot{x}_b|} \quad (4)$$

where the parameters $\mu_{\min}$, $\mu_{\max}$ and a are functions of bearing pressure, surface roughness of stainless steel and composition of Teflon.

The simplest model is the Coulomb type which will be used in this study for simplicity in common with most of the researches which were carried out in recent years [3,10–16,23,28,29,45].

5. Model validation by experimental data

In order to show the validity of the model of the bearing presented above, behavior of the assumed numerical model is compared with past experiments on set of sliders and sliding plates with configuration similar to the multiple-slider bearing [21,30], except that the location of the PTFE sliders and stainless steel sliding plates are inverted Fig. 4.

The tests apparatus for the tests is shown in Fig. 5. A weight of 18 kN is installed on the top of the upper component. The PTFE dimensions used are 100 × 100 mm and 50 × 200 mm for the horizontal and inclined surfaces, respectively, and the clearance of 180 mm is used for all cases. Sinusoidal displacements of amplitude 250 mm with various velocity rates are applied to the lower component of the specimen.

Fig. 6 shows the hysteresis behavior of the specimen with inclination angle $\theta = 30°$ at velocity rate of 1.6 cm/s. It is obvious that the hysteresis behavior resembles the simplified proposed model in Fig. 3. Applying Eq. (3) with μ about 0.14, the lower and upper bound of the horizontal forces generated at the inclined surfaces i.e. 14 kN and 7 kN are found similar to the force level shown by the dashed lines and these confirm the right formulation of the displacement–force relationship.

The effect of excitation at higher velocity is illustrated in Fig. 7 for $\theta = 15°$. It can be concluded from Fig. 7 that there are some differences especially in cases where excitation velocity is high due to impact forces that are generated at the transition point between sliding surfaces. The test results indicate that higher θ generates higher impact force. As mentioned earlier, the hysteresis curve shown in Fig. 3 is still regarded as a good approximation that covers the essential characteristics of the device, and is used in the re-

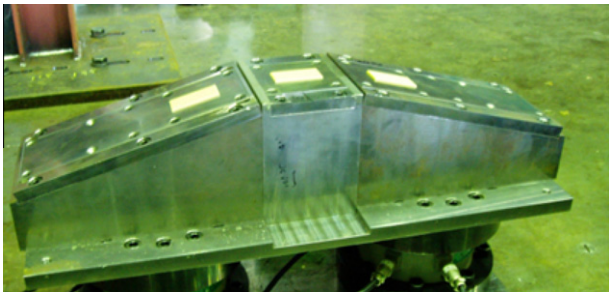

Fig. 4. Lower component of the test specimen with PTFE pads.

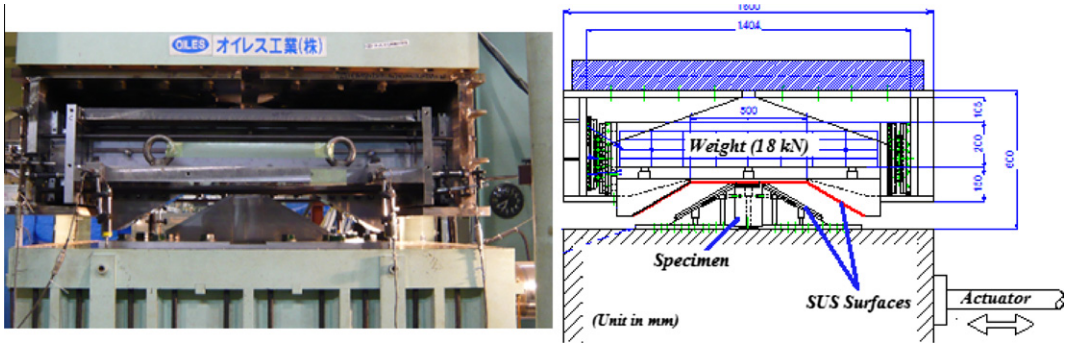

Fig. 5. Details of test experiment.

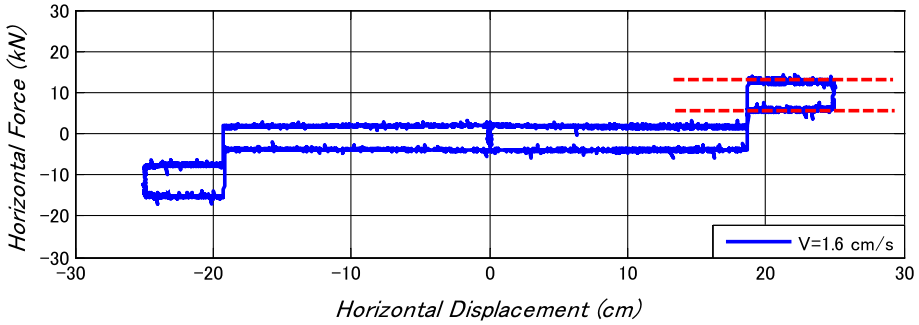

Fig. 6. Hysteresis behavior of bearing with $\theta = 30°$.

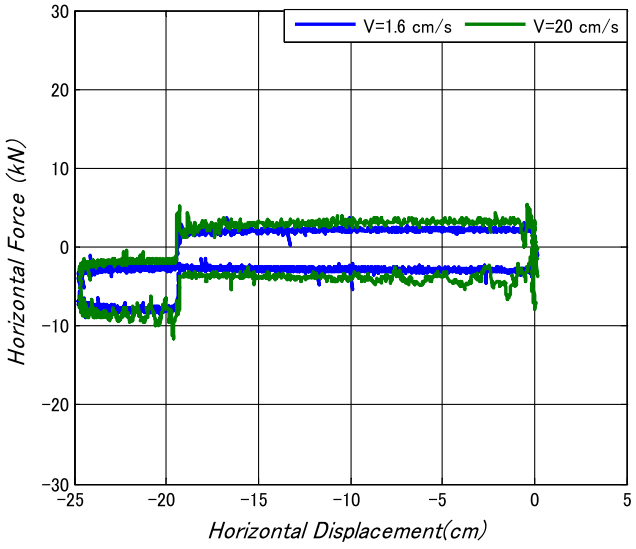

Fig. 7. Hysteresis behavior of bearing with $\theta = 15°$ at different velocity rate.

sponse analysis of the system in this study to simplicity of the analysis.

6. Numerical example: four-story shear-type building

The dynamic response of a flexible superstructure supported on the multiple-slider bearing system under earthquake motion is investigated and compared with the rubber bearing isolation system as well as pure friction sliders. The sliding devices are repeatedly subjected to transition phases between stick and slip modes, which introduces discontinuity and high nonlinearity. One of the most efficient methods which have been proposed for solving the

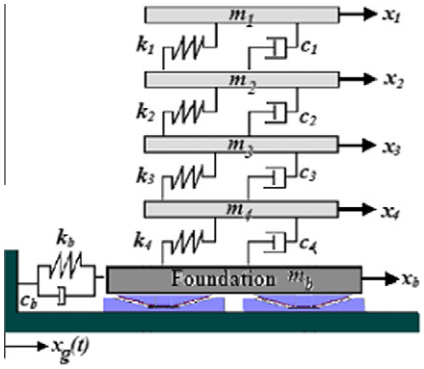

Fig. 8. Four-story shear-building isolated by multiple-slider bearings.

discontinuities occurring in analysis of sliding structure is the fictitious spring approach [13]. By this method, a fictitious spring is introduced between the base mat and the ground to represent the mechanism of friction. The fictitious spring stiffness (k_f) is taken as zero for the sliding phase and as sufficiently large number for the non-sliding phase. This assumption is suitable with the mechanism of the sliding device, since Teflon-steel interfaces undergo some very small elastic displacement before sliding, partly due to small elastic shear deformation of the Teflon material [27].

For the purpose of illustration, four-story shear-type building as shown in Fig. 8 will be studied.

The properties of the model are chosen to be identical to a model described in reference [13]. It is assumed that story masses are equal so that $m = 350.2$ kg and the mass of the foundation $m_f = 4m/3$ and stiffness for all stories are set equal to $k = 573.6$, 103 N/m. Rayleigh damping is used to formulate the damping matrix. It has been assumed that the damping ratios ζ for the first two modes of vibration equal to 5%. The fundamental period of the

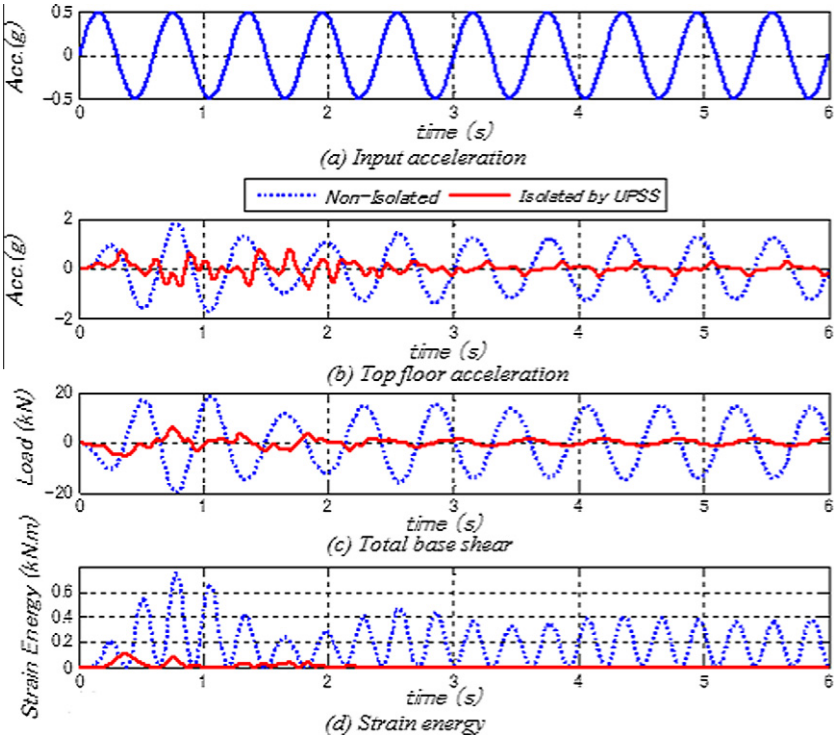

Fig. 9. Comparison of non-isolated and isolated buildings.

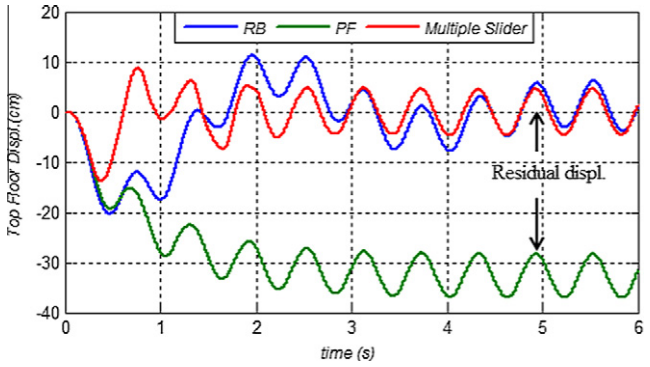

Fig. 10. Comparison of top floor displacements with RB, PF and multiple-slider bearings.

fixed base building T_1 is 0.447 s. The multiple-slider bearing properties have been chosen with $L = 45$ mm and $\theta = 10°$. The RB has chosen to give a period of isolation T_b of 3.0 s and the effective damping ratio ζ_b equal to 10%. The RB is a mean of providing a displacement restrain. Therefore, the total stiffness of RB is assigned as $k_b = 8320$ N/m to achieve the desired isolation period. The dominant property of RB is the parallel action of linear stiffness and damping.

The restoring force (F_b) of RB has been modeled with a linear force–displacement relationship with viscous damping and can be expressed as follows:

$$F_b = k_b x_b + c_b \dot{x}_b \tag{5}$$

and

$$c_b = \zeta_b \times (2\omega_b m_t) \tag{6}$$

where c_b is the effective viscous damping coefficient of RB; m_t is the total mass of the superstructure including the foundation; ω_b is the angular isolation frequency i.e. $\sqrt{\frac{k_b}{m_t}}$.

The friction coefficient of the multiple-slider bearing for all the three sliding surfaces μ is assumed to be 0.05. The superstructure is assumed to behave elastically linear which is compatible with the main purpose of base isolation and the overturning or tilting effect of the structure during sliding has been neglected.

7. Simulation results

To verify the effectiveness of the isolator as a new promising alternative for seismic isolation sliding devices, reduction of two main response quantities, namely, the isolator displacement x_b and the top absolute floor acceleration $\ddot{x}_a$, is the main concern. In order to clarify the advantage of the proposed device, the comparison with responses of the isolated building by RB and PF are also considered.

The structure is subjected to harmonic sinusoidal excitation with intensity taken as 0.50 g high enough to insure sliding and uplift mechanism in the multiple-slider bearing and the period of excitation T_g taken as 0.6 s; a typical value sufficient smaller than T_b. Only unidirectional excitation is considered.

The simulation results shown in Fig. 9 demonstrate the efficiency of the multiple-slider bearing in comparison with the non-isolated building. The maximum absolute top floor acceleration has been reduced significantly from 1.81 g to 0.77 g, which means a reduction of about 60%, as shown in Fig. 9b. The small peaks seen in the acceleration time history are generated by the slip–stick action due to the sudden changes in the friction force value in the transition sliding phases which exerts shock impulses on the support. It is clearly indicated in Fig. 9c and d that multiple-slider bearing efficiently suppresses load transmitted into the superstructure, as well as the total base shear and strain energy.

From the comparison with RB and PF isolation systems shown in Fig. 10, the maximum top floor displacement for the multiple-slider bearing case has been found to be less than that for both RB and PF systems. This shows the effectiveness of this device in controlling the peak displacement values to acceptable limits,

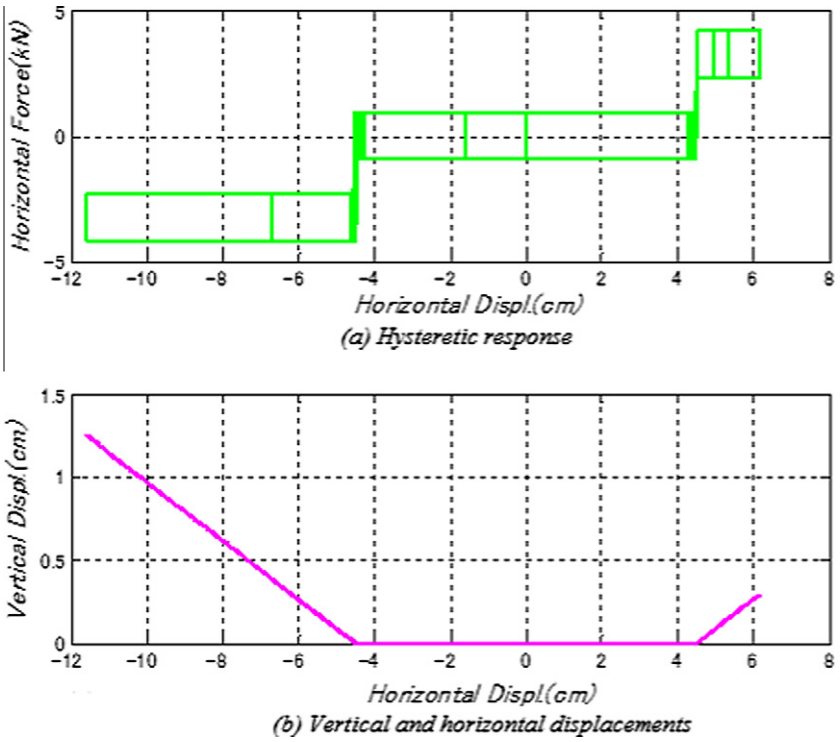

Fig. 11. Hysteresis loop for the multiple-slider bearing.

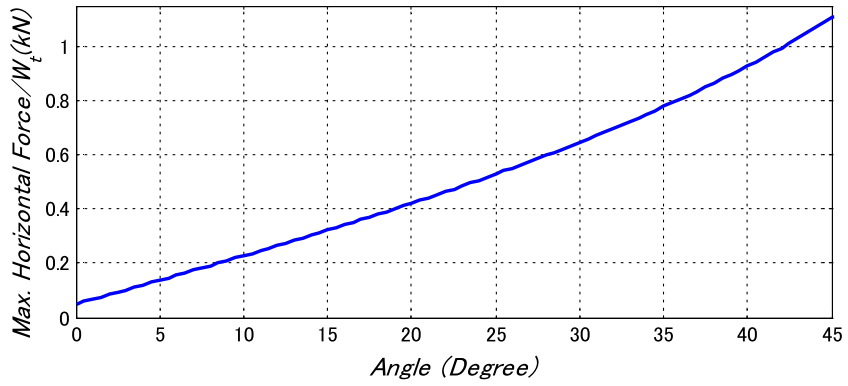

Fig. 12. Maximum base shear to total weight ratio and the variation in the inclination angle for $\mu = 0.05$.

being one of the most important reasons to consider the bearing as a good alternative to solve the problem of large displacement of the RB and the residual displacement of the PF isolation system. The maximum displacement of the multiple-slider bearing isolator can be further reduced by a better selection of the three main parameters that define the device L, θ and μ as indicated by sensitivity analysis for these three parameters and their effect on the dynamic behavior described in the next section of this paper.

The dynamic characteristics of the multiple-slider bearing system under seismic excitation are illustrated by the response shown in Fig. 11. The enclosed area in the hysteretic force–displacement relationship Fig. 11a represents the portion of the energy dissipated by the friction mechanism. The hysteretic behavior indicates that after the displacement exceeds the clearance length, the uplift mechanism is activated to convert some of the kinetic energy to a potential one and to control the horizontal displacement, as can be noticed from the trace graph that depicts the relationship between the horizontal and vertical displacements in Fig. 11b.

Design codes require that the isolation system should be able to provide restoring forces to bring the isolation device back to its original position prior to engagement. For example, the 1991 AASHTO Guide Specifications for Seismic Isolation Design [31], require that the difference between the magnitude of the restoring force at design displacement and at 50% of the design displacement is larger than 2.5% of the tributary weight acting on the isolation bearings. For cases where this criterion is not met, the isolation system must be capable of accommodating displacements equal to the greater of three times the displacement calculated by the single mode analysis method, or $36AS_i$ inches, where A and S_i are the acceleration and site coefficients, respectively. The 1999 AASHTO Guide Specifications [32] limit the post-elastic period to a maximum of 6 s. In the same manner, ASCE 7-05 [33] and Eurocode 8 [34] states that an isolation unit should be capable of producing a value 2.5% multiplied by the seismic weight, greater than the lateral force at 50% of the total design displacement, in order to restore the isolator to its original intended position.

The unique fundamental dynamic behavior of the multiple-slider bearing is based on the geometry of the bearing that allows vertical movement through the sliding along the inclined surface. On the contrary of the friction pendulum system (FPS) which uti-

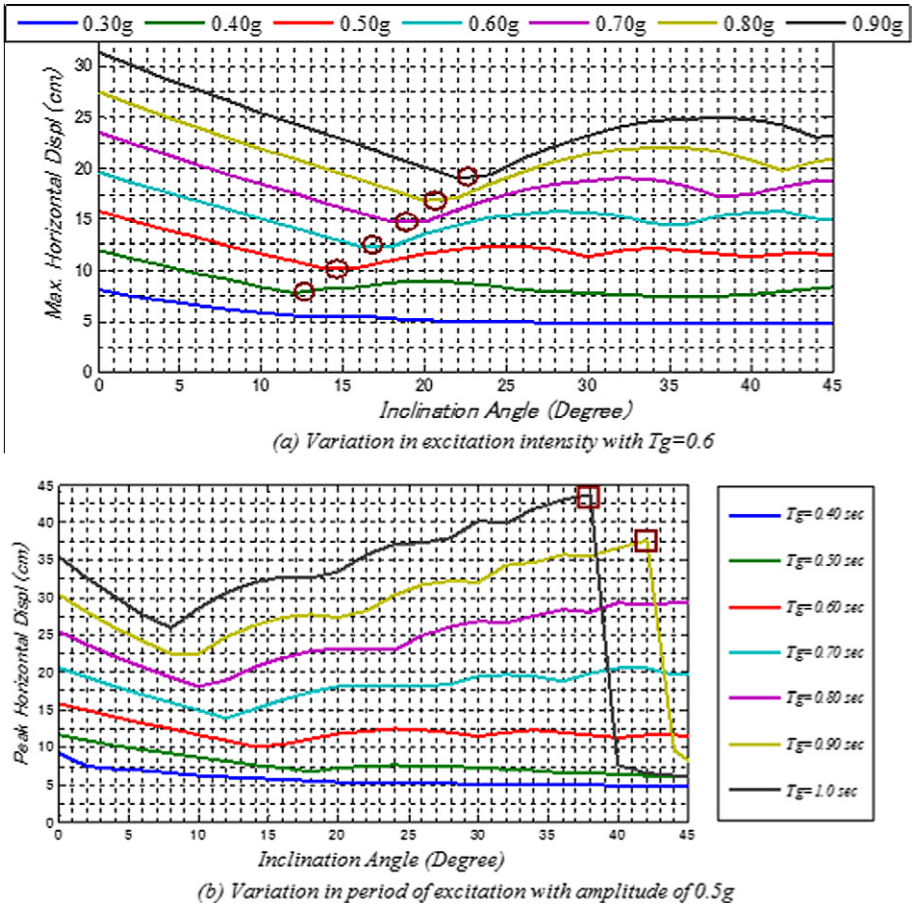

Fig. 13. Maximum base horizontal displacement verses inclination angle.

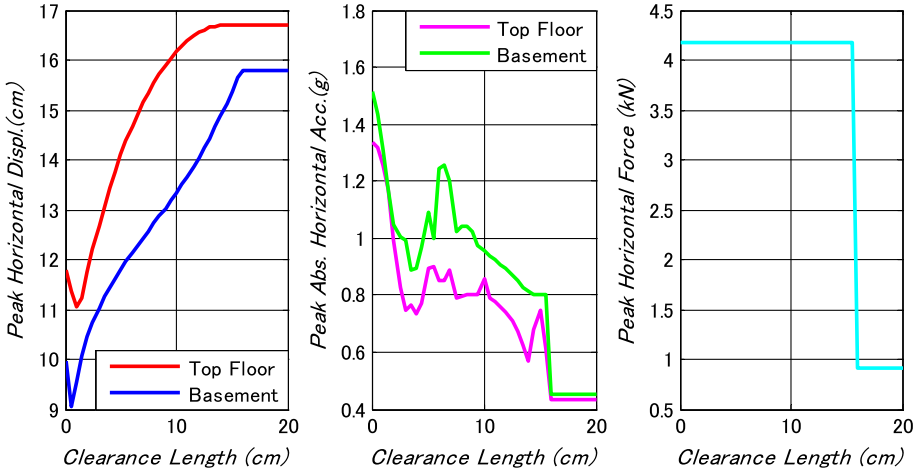

Fig. 14. Clearance length vs. peak responses for the shear-type building.

lizes a spherical sliding surface to develop a restoring force, the slope angle of the inclined surfaces in the multiple slider bearing is much larger than the range of the tangential angles of the sliding surfaces of FPS, so that the vertical component of the structural motion is explicitly intended and a constant restoring force is generated due to the component of self-weight tangent to sliding surfaces. Fig. 10 affirms the fact that the multiple-slider bearing inherit a self-centering mechanism in contrast with the pure slider (PF) which lacks the capability to return to the original position. However, to insure more safety conventional rubber bearing has been used in the numerical model as a mean of providing a displacement restrain, see Fig. 8.

8. Parametric study

A properly designed base isolation is accomplished by understanding the sensitivity of the device parameter values and their influence on the structural response. In this section, the characteristics of the multiple-slider bearing with respect to the maximum

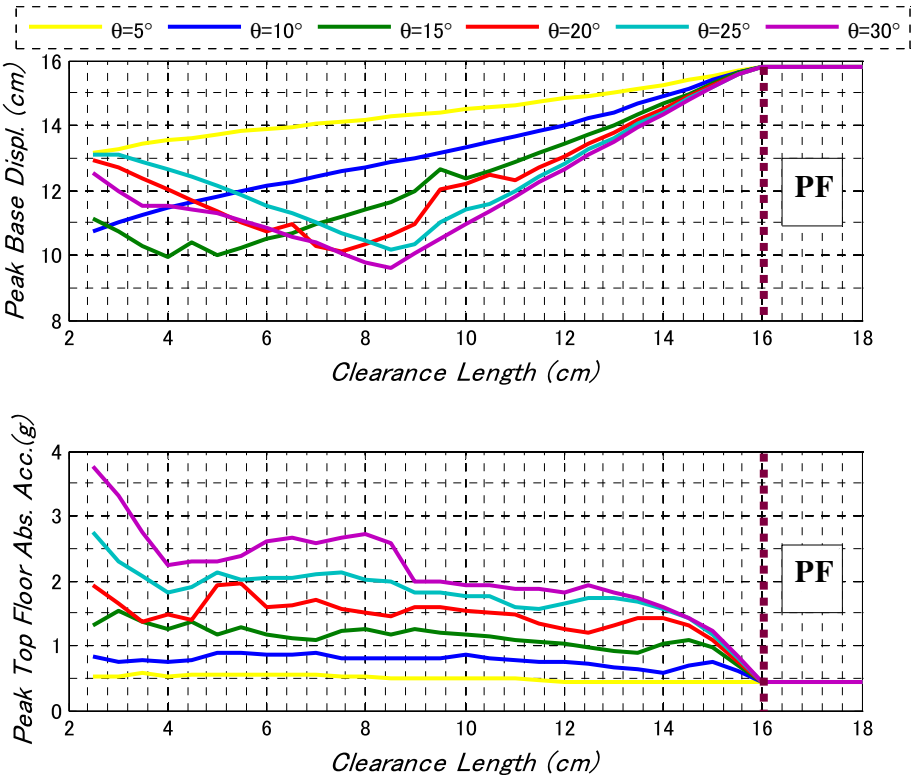

Fig. 15. Clearance length vs. spectra responses under various inclination angles.

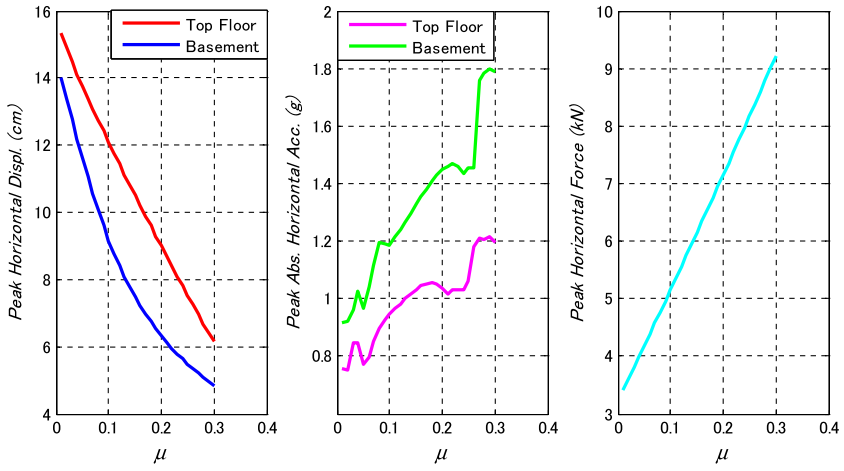

Fig. 16. Friction coefficient vs. peakresponses.

horizontal displacement and base shear are examined with the variation of L, θ and μ. The identical example model of the four-story shear-type building under the sinusoidal excitation is used for the analysis.

8.1. The inclination angle (θ) effect

The isolator displacement is the main concern in the analysis described in this section. The relationship between the maximum base shear to total weight ratio and the variation in the inclination angle for $\mu = 0.05$ is shown in Fig. 12, which is obtained directly from Eq. (3) that depends on the inclination angle and the coefficient of friction. For practical purposes, the maximum angle was set equal to 45°. The increase in the sliding angle will lead to an increase in the horizontal force as indicated in Fig. 12, resulting in an increase in the total base shear and the floor acceleration. The effect of variation of the inclination angle on the base floor horizontal displacement is shown in Fig. 13. The effect is also examined under various excitation intensities and periods of excitation. The isolated shear type building was subjected to excitation intensity up to 0.90 g and period of excitation up to 1.00 s.

For low intensity input up to 0.4 g, changing the angle does not significantly affect the maximum peak base displacement. However, for moderate to high intensity earthquakes exceeding 0.5 g, the increase in the inclination angle is clearly effective in reducing the displacement demand. It is observed that there is an optimum angle for each case that gives the least minimum displacement, the higher the intensity the higher this optimum angle. A small circle is

added to indicate these optimum values. The effect of the variation in the excitation frequency is shown in Fig. 13b. For periods of excitation 0.4 s and 0.5 s, a gradual reduction in the peak horizontal displacement occurs with the increase in the inclination angle. Nevertheless, for longer periods exceeding 0.6 s, the reduction occurs up to a certain limit then starts increasing. For the periods of 0.9 and 1.0 s, there exists a point where any further increase in the inclination angle would induce a sudden drop in the peak horizontal displacement and keep its value constant equal to the clearance length. This turning point, which is marked by a small square, can be seen as the maximum angle for each period of excitation in which uplift mechanism cannot be developed further more. It is obvious that this angle is reached faster for long periods than shorter periods of excitation.

8.2. Clearance length (L) effect

To acquire a better understanding for L length on the structural response, the same four-story shear-building is used for the numerical calculation. L is been selected varies up to 20 cm. The captured response quantities of interest are the maximum top and base floor displacements and acceleration, as well as the maximum horizontal force, as shown in Fig. 14.

It is clearly shown by this graph that the longer the clearance length, the higher the peak displacement and the lower the absolute peak acceleration. The peak horizontal force is unchangeable with the change of clearance length since this mechanism of the multiple-slider bearing depends only on the inclination angle, the coefficient of friction and the total weight. The sudden drop in the restoring force indicates that the peak horizontal displacement is less than the clearance length which means the system truly behaves like a pure friction device without the uplift mechanism. It is obvious that using smaller clearance length may cause large reduction in the horizontal displacement but in the expense of higher top absolute acceleration. The designer should choose adequately what the priority in the design is in term of cost and space limitations.

For a deeper understanding and clearer representation, Fig. 15 is established to relate simultaneously both the variation of clearance length and angle of inclination with two quantities of interest; the peak base displacement and top absolute peak acceleration. From Fig. 15, it is recommended to adopt a small angle of inclination when dealing with a small clearance length to avoid the high acceleration of top floor since such configuration may not allow the isolator to absorb the shock efficiently through the plane sliding part.

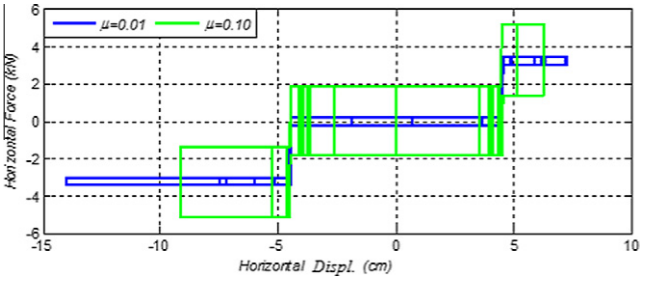

Fig. 17. Hysteresis loop for UPSS for two different friction coefficient values.

8.3. Friction coefficient effect

In this section, the effect of the friction coefficient is investigated. As stated before, the multiple-slider bearing possesses a distinguishing feature that permits the use of variable friction coefficients. Therefore, the following discussion is divided into two cases: equal and non-equal friction coefficient cases. Several different friction coefficients ranging from 0.01 to 0.3 are considered in each case.

8.3.1. Equal friction (μ)

Equal friction implies that the same sliding material is used for the three sliding surfaces in both the horizontal and inclined planes. To illustrate the effect of the friction coefficient values, the peak responses of the isolated superstructure and the isolator horizontal force vs. the variation of friction coefficient values are shown in Fig. 16.

It is observed that for smaller μ values, reduction in acceleration is more efficient accompanied with a higher peak displacement. In order to clearly show the difference in response behavior for different friction coefficient values, the hysteretic loops for two μ values of 0.01 and 0.10 are plotted in Fig. 17. It is obvious that the friction coefficient strongly controls the shape of the hysteretic curve; the lower the value, the narrower band dissipation system with more softener mechanism is generated i.e. larger displacement and lower force.

The influence of loading characteristics such as the intensity and period of excitation and its relationship with the friction coefficient on the peak base horizontal displacement and the peak top floor absolute acceleration is traced and plotted in Figs. 18 and 19. Both diagrams clearly depict that the friction coefficients in all cases of excitation are approximately inversely proportional to

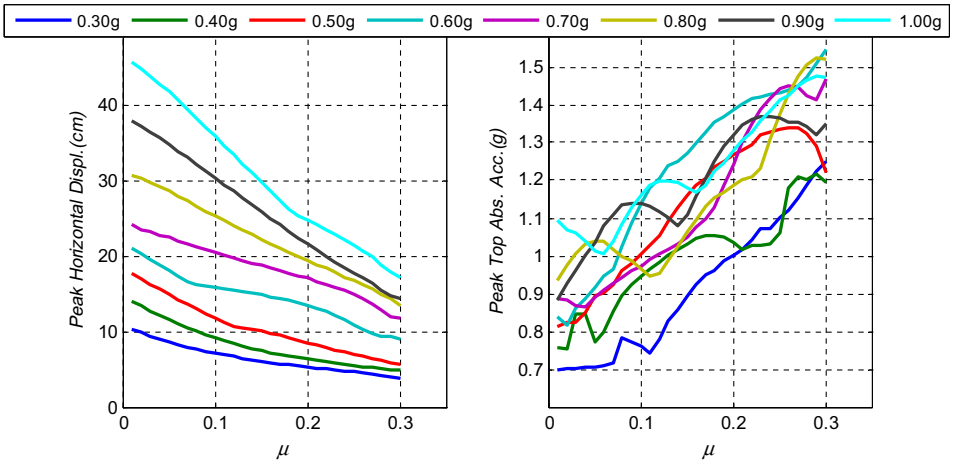

Fig. 18. Relationship between peak response and friction coefficient with respect to T_g = 0.6 s.

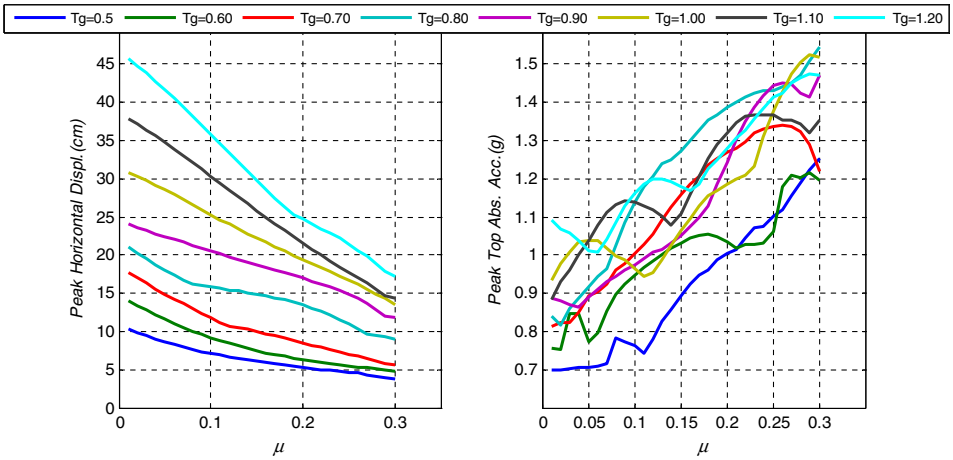

Fig. 19. Relationship between peak response and friction coefficient at amplitude of 0.5 g.

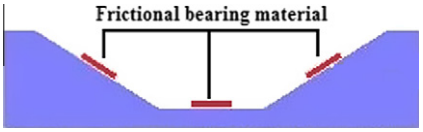

Fig. 20. Locations of frictional bearing material in the multiple-slider bearing.

the peak horizontal base displacement. On the other hand, the peak top absolute acceleration tends to increase with the increase of response with the increase of the friction coefficient. It is should be noted that for small friction coefficients, the top acceleration is not significantly affected by excitation intensity variation.

8.3.2. Non-equal friction (μ_1 and μ_2)

The geometry of multiple-slider bearing inherits a distinctive advantage that offers the ability to use different friction coefficients for each sliding surface, as seen in Fig. 20. The use of such non-equal friction coefficients is expected to be helpful to control the isolator displacement.

Some researchers have investigated theoretically the effectiveness of varying the friction coefficient within the FPS by gradually varying the roughness of the spherical surface [35]. Such variation is selected with the criterion that the isolator displacement and building base shear decrease significantly without much alteration to superstructure acceleration. In this section, an investigation of using different sets of friction coefficient for each sliding surface is performed. The plane sliding surface is assumed to have a friction coefficient (μ_1) and the two inclined surfaces are assumed to have the same friction coefficient (μ_2) for symmetry and practical purposes.

Many researches showed that that isolated structures may be susceptible to near-fault ground motions such that the demand imposed by their displacement pulses can exceed the capacity of the isolators designed to current standards [19,36–38]. These ground-displacement pulses are associated directly with the fault-rupture process and can cause considerable damage to flexible structures. Such ground motions may have one or more displacement pulses ranging from 0.5 m and higher with peak velocity of 1 m/s or greater. The presence of long-duration pulses has a large impact on isolated structures which requires a large displacement to be accommodated by the isolators, which may be excessively greater than a practically feasible value in engineering design. Some researchers suggested the use of a passive isolation system combined with a semi-active control device to

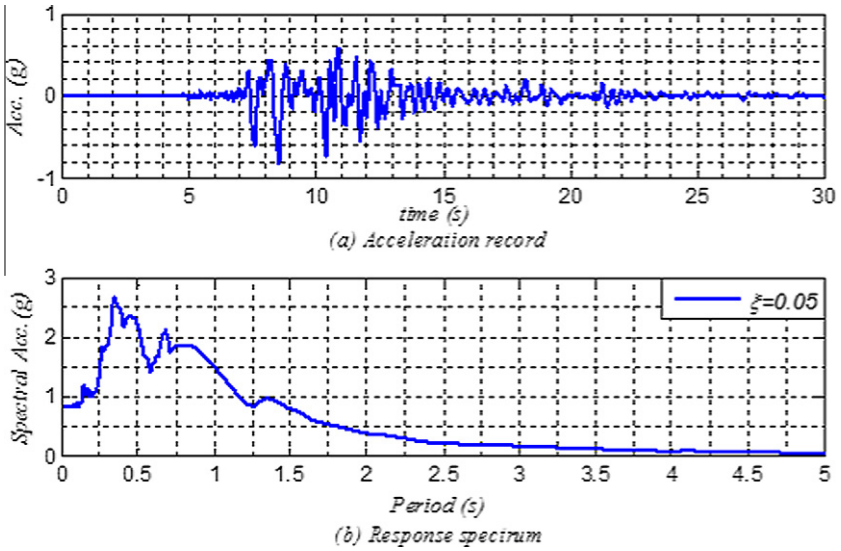

Fig. 21. 1995 Hanshin Kobe earthquake JMA record NS component.

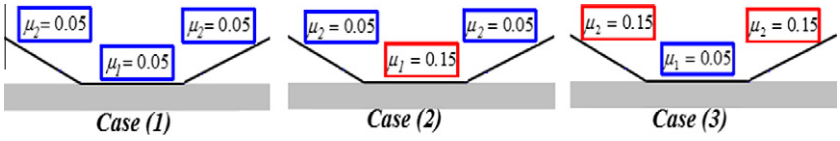

Fig. 22. Free diagram of bearings: equal and nonequal friction coefficient at $L = 45$ mm, $\theta = 10°$.

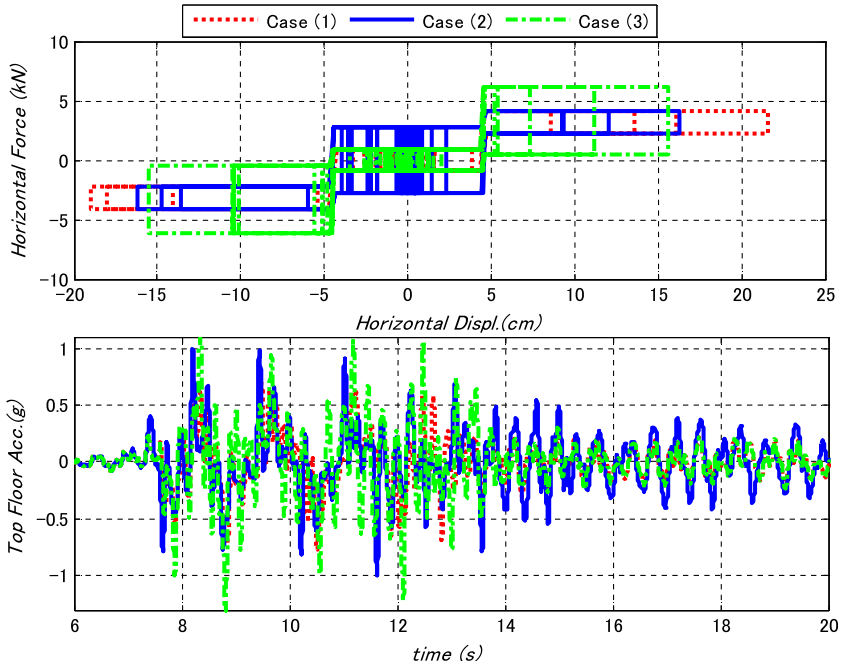

Fig. 23. Comparison of responses for equal and nonequal multiple-slider bearing subjected to Kobe earthquake.

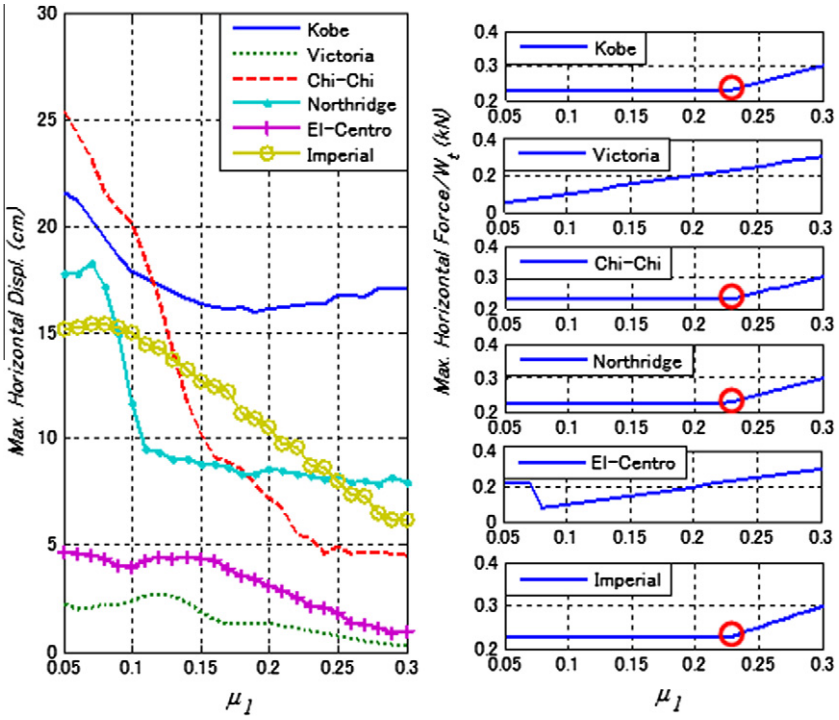

Fig. 24. Relationship between μ_1 and maximum displacement and force under various earthquake ground motion records.

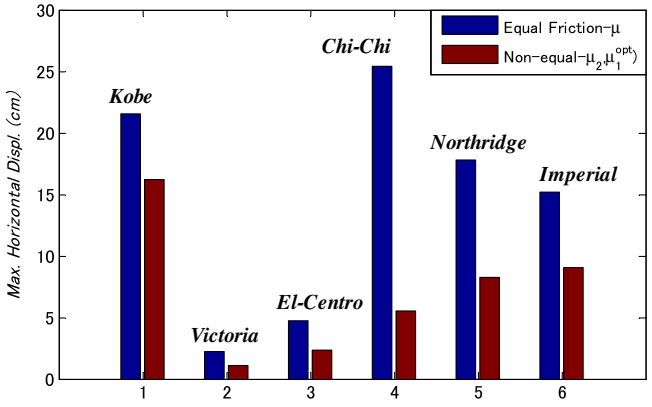

Fig. 25. Comparison between equal and non-equal friction under various earthquakes.

enhance the safety of near fault structures [44]. The most common solution is the use of supplementary dampers to reduce such effect, on the expense of increasing the cost, the inter-story drift and floor superstructure acceleration [35].

The multiple-slider bearing has a high potential in controlling and minimizing the effect of the ground displacement pulses represented primarily through its operation mechanism. It will be shown that varying the friction coefficient also helps to maximize the efficiency of the bearing by reducing the displacement response especially in the cases of strong and near fault motions.

In order to study the dynamic behavior of the base-isolated shear type building with non-equal friction, 1995 Hanshin Kobe earthquake JMA record is used, see Fig. 21. The Kobe earthquake record has peak ground acceleration of 0.83 g, and duration of ground motion is considered to be 30 s. The same four-story shear type-building is used for this purpose, and the results are also compared with the equal friction coefficient bearing case.

Three cases of equal and non-equal friction bearing material, shown in Fig. 22, are used first to determine whether the larger friction coefficient value should be placed at the plane surface or the inclined surface part to achieve a more reduction in horizontal displacement. The simulation results and the comparison between equal and non-equal bearings are shown in Fig. 23.

It can be concluded from Fig. 23 that for a better performance, the friction coefficient of plane surface should be taken larger than the friction coefficient of the inclined surface as in case (2). Contrary to case (3), case (2) can induce noticeable reduction in the maximum isolator displacement without any change in the maximum horizontal isolator force. However, this reduction may cause some increase in the top acceleration response due to the higher yielding frictional level in the plane surface which leads to a longer duration in the stick phase. The hysteresis behavior of the bearing indicates a significant reduction in the isolator peak horizontal displacement. The peak isolator displacement is efficiently reduced by 25% in case (2) using the non-equal friction coefficient.

Further investigation for the effect of varying the plane surface friction coefficient μ_1 on the maximum horizontal bearing displacement and horizontal force is carried out using several ground motion records. The earthquake ground motions considered are:

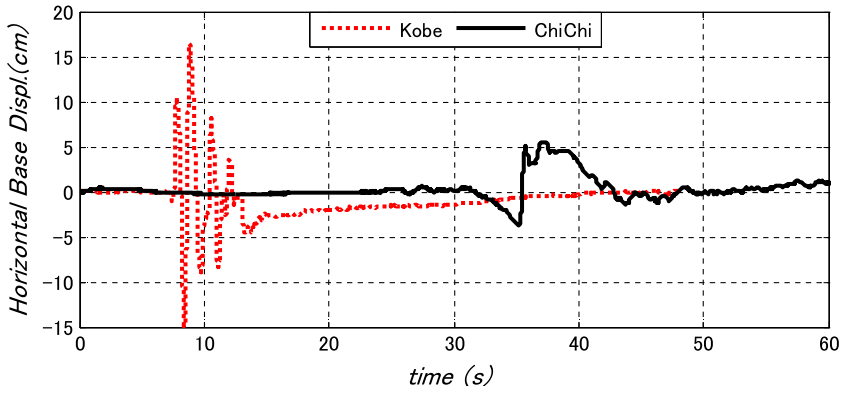

Fig. 26. Displacement and acceleration time history ($L = 45$ mm), $\theta = 10°$, $\mu_1^{opt} = 0.228$, $\mu_2 = 0.05$).

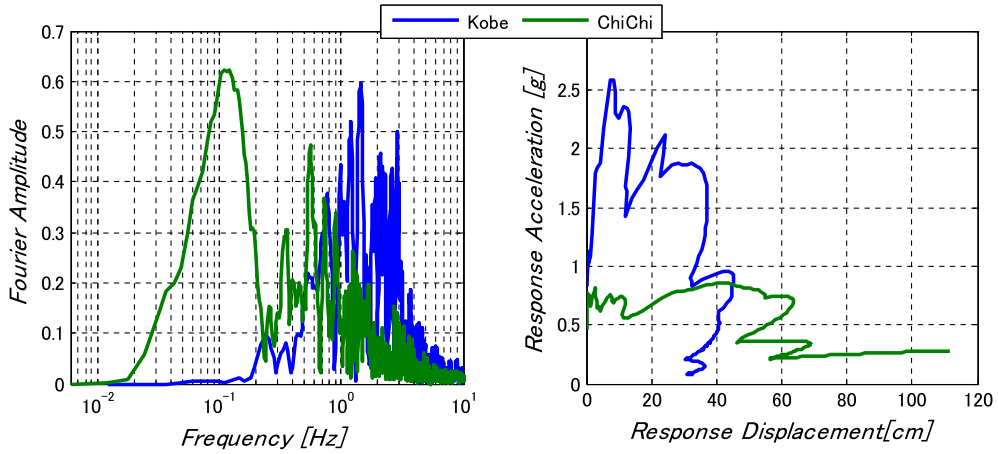

Fig. 27. Fourier and spectrum analysis for Kobe and Chichi earthquakes.

(1) 1995 Hanshin Kobe record (PGA = 0.82 g); (2) 1980 Victoria, Mexico record (PGA = 0.59 g); (3) 1940 El-Centro record (PGA = 0.32 g); (4) 1999 Chichi-TCU-068 record (PGA = 0.46 g); (5) 1994 Northridge record (PGA = 0.60 g); (6) 1979 Imperial Valley, El-Centro Array #7 record (PGA = 0.62 g). The above model is used with bearing properties of L = 45 mm, $\theta = 10^\circ$ and $\mu_2 = 0.05$. The simulation results are shown in Fig. 24. The trend of horizontal displacement response curves reaffirms the above stated fact that a higher friction coefficient μ_1 leads to a higher reduction without any increase in the horizontal force up to a certain point where forces start increase. A small circle is added to these points. For some earthquakes such as Victoria and El-Centro records, although there is still a displacement reduction, it is observed that the force pattern is different than that of the rest earthquake record responses. The reason behind this pattern in the case of Victoria record is due to earthquake wave characteristics that are not able to develop the uplift mechanism and all displacement responses are less than the clearance length for all combinations of μ_1.

Therefore, the linear increase of the horizontal force shown in Fig. 24 is due to the frictional force limit in the plane horizontal surface of the multiple-slider bearing proportioned to μ_1. As for El-Centro record, the forces kept constant until μ_1 reaches about 0.07 in which further increase in μ_1 prevents the development of uplift mechanism and the behavior continue similar to Victoria record.

It is clear that the point marked earlier can be considered as an optimum point in term of achieving a maximum displacement reduction without any change in the horizontal force. This point represents the value of μ_1 that produces a frictional yielding limit in the plane surface equal to that developed in the inclined surface. Based on Eq. (3), the optimum value μ_1^{opt} can be calculated as:

$$\mu_1^{opt} = \left[\frac{+\mu_2 \cos\theta + \sin\theta}{-\mu_2 \sin\theta + \cos\theta}\right] \tag{7}$$

Applying this formula to our example model the optimum μ_1^{opt} is equal 0.228 which matches with the same value in Fig. 24. Comparison of equal friction case ($\mu = 0.05$) and non-equal friction case ($\mu_1^{opt} = 0.228$, $\mu_2 = 0.05$) under the various earthquake excitations is plotted in Fig. 25. This plot shows the high efficiency of using non-equal friction with an optimum value to achieve a large reduction up to 78% of the equal friction case as in Chichi earthquake.

The remarkable performance in Chichi earthquake case compared with Kobe earthquake as shown in Fig. 26 is the result of the unique characteristics of each seismic wave. Fig. 27 also shows the Fourier and spectrum analysis comparison between these two records. The analysis of these two near fault ground waves indicates that Kobe record exhibits forward directivity effect while Chichi record exhibits fling-step effect. The forward directivity is characterized by a large pulse occurring at the beginning of the motion to be oriented in a direction perpendicular to the fault plane while the fling-step is the outcome of the tectonic permanent deformation oriented parallel to the fault [39–41]. The destructive potential of the permanent displacements of Chichi waves caused by the fling-step effect has been successfully absorbed and cut off through the response mechanism of the non-equal friction multiple-slider bearing causing such a significant displacement reduction more obvious than in Kobe earthquake case.

9. Conclusions

The multiple-slider bearing is introduced to enhance the seismic performance of multi-story structures and to reduce the horizontal displacement with a low cost. The multiple-slider bearing is composed of three sliding surfaces based on the PTFE and stainless steel interface; one horizontal and two inclined surfaces. A simplified mathematical model is used to represent the mechanical behavior and the underlying principles of operation. The dynamic response of a flexible superstructure supported on the multiple-slider bearings system under earthquake motion is investigated and compared with rubber bearing and pure friction slider systems. Preliminary analysis on the influence of the variation of clearance length, the inclination angle and the friction coefficient on the response of multistory building and the unique feature of the multiple-slider bearing that permits the use of different friction coefficients is investigated. Based on the presented study, the following conclusions can be drawn:

1. Simulation results indicate that the newly proposed bearing is more effective in mitigating the risk of earthquake and preserving multi-story buildings from damage than the conventional rubber bearing and the pure friction slider in term of peak horizontal displacement.
2. Higher inclination angle is effective in reducing horizontal displacement especially in moderate to high excitation intensities but on the expense of higher forces. It was observed that there is an optimum angle that gives a minimum horizontal peak displacement and it depends on the excitation characteristics and structure properties.
3. The analysis indicates that the longer the clearance, the higher the peak displacement and the lower the absolute peak acceleration.
4. The peak horizontal displacement is approximately inversely proportional to the friction coefficient with all cases of excitation. It is also observed that for small friction coefficients, the top acceleration is not significantly altered with changing excitation intensity.
5. The geometry of the multiple-slider bearing inherits a distinctive advantage that offers the ability to use different friction coefficient for each sliding surface. This lead the bearing to possess a high potential in controlling and minimizing the peak horizontal displacement in addition to its primary reduction through the mechanism of uplift.
6. It has also been found that for a better performance of the proposed bearing, the friction coefficient of the horizontal plane surface should be taken larger than the friction coefficient of the inclined surface. Besides, there is an optimum friction value that causes a high displacement reduction without any change in the horizontal force and the principle to define the optimal value is developed.

Acknowledgements

The authors would like to express their gratitude towards Mr. Hiroshige Uno of Oiles Corporation, Dr. Yukio Adachi of Hanshin Expressway Corporation, Mr. Tomoaki Sato, Mr. Yoshihisa Kato, and Mr. Yasuyuki Ishii for their valuable advice, support and suggestions on this research.

References

[1] Buckle I, Mayes R. Seismic isolation: history, application and performance a world overview. Earthquake Spectra 1990;6(2):161–202.
[2] Skinner R, Robinson W. An introduction to seismic isolation. England: John Wiley; 1993.
[3] Su L, Ahmadi G, Tadjbakhsh IG. A comparative study of performance of various base isolation systems, Part I: shear beam structures. Earthquake Eng Struct Dynam 1989;18:11–32.
[4] Jangid R, Data TK. Seismic behavior of base isolated buildings-A state-of-the art-review. J Struct Build 1995;110:186–203.
[5] Kunde MC, Jangid RS. Seismic behavior of isolated bridges: a state-of-the-art review. Electron J Struct Eng 2003;3:140–70.

[6] Qamaruddin M. A-state-of-the-art-review of Seismic Isolation Scheme for Masonry Buildings. ISET J Earthquake Technol 1998;35(4):77–93 [paper no. 376].
[7] Earthquake Protection Systems. Technical characteristics of friction pendulum bearings. Vallejo, California; 2003.
[8] Kawamura S, Kitazawa K, Hisano M, Nagashima I. Study of a sliding-type base isolation system – system composition and element properties. In: Proceedings of 9th WCEE, Tokyo-Kyoto, vol. 5; 1988. p. 735–40.
[9] Watson RJ. Sliding isolation bearings in cold weather climates. In: Mahmoud Khaled M, editor. Innovations in bridge engineering technology. London: Taylor and Francis Group; 2007. p. 103–10.
[10] Westermo B, Udwadia F. Periodic response of a sliding oscillator system to harmonic excitation. Earthquake Eng Struct Dynam 1983;11:135–46.
[11] Mostaghel N, Tanbakuchi J. Response of sliding structures to earthquake support motion. Earthquake Eng Struct Dynam 1983;11:729–48.
[12] Younis CJ, Tadjbakhsh IJ. Response of sliding rigid structure to base excitation. J Eng Mech 1984;110:417–32.
[13] Yang YB, Lee TY, Tsai IC. Response of multi-degree-of-freedom structures with sliding supports. Earthquake Eng Struct Dynam 1990;19:739–52.
[14] Vafai A, Hamid M, Ahmadi G. Numerical modeling of MDOF structures with sliding supports using rigid-plastic link. Earthquake Eng Struct Dynam 2001; 30:27–42.
[15] Lu L, Yang Y. Dynamic response of equipment in structures with sliding support. Earthquake Eng Struct Dynam 1997;26:61–77.
[16] Mostaghel N, Khodaverdian M. Dynamics of resilient-friction base isolator (R-FBI). Earthquake Eng Struct Dynam 1987;15:379–90.
[17] Su L, Ahmadi G, Tadjbakhsh IG. Performance of sliding resilient friction base isolation system. J Struct Eng 1991;117:165–81.
[18] Zayas V, Low S. A simple pendulum technique for achieving seismic isolation. Earthquake Spectra 1990;6(2) [Earthquake Engineering Research Institute, Oakland, California].
[19] Paresh M, Sinha Ravi. VFPI: an isolation device for aseismic design. Earthquake Eng Struct Dynam 2000;29:603–27.
[20] Igarashi A, Sato T, Shinohara M, Katou Y, Uno H, Adachi Y et al. Uplifting slide bearing (1) – characterization of dynamic properties. In: 34th IABSE symposium on large structures and infrastructures for environmentally constrained and urbanised areas, Venice, Italy; 2010.
[21] Igarashi A, Sato T, Shinohara M, Katou Y, Uno H, Adachi Y. Uplifting slide bearing (2) – verification of seismic response by tests. In: 34th IABSE symposium on large structures and infrastructures for environmentally constrained and urbanised areas, Venice, Italy; 2010.
[22] Igarashi A, Sato T, Shinohara M, Katou Y, Uno H, Adachi Y. Uplifting slide bearing (3) – development of the analytical model. In: 34th IABSE symposium on large structures and infrastructures for environmentally constrained and urbanised areas, Venice, Italy; 2010.
[23] Igarashi A, Sato T, Shinohara M, Katou Y, Uno H, Adachi Y. Uplifting slide bearing (4) – application for a 3-span steel girder. In: 34th IABSE symposium on large structures and infrastructures for environmentally constrained and urbanised areas, Venice, Italy; 2010.
[24] E.I. du Pont de Nemours & Co. Teflon: Mechanical design data. Wilmington, DE; 1981.
[25] Mokha A, Constantinou M, Reinhorn A. Teflon bearing in base isolation I: testing. J Struct Eng 1990;116(2):438–54.
[26] Costantinou MC. Design and applications of sliding bearings. In: Soong TT, Costantinou MC, editors. Passive and active structural vibration control in civil engineering. New York: Springer, Wein; 1994. p. 111–35.
[27] Constantinou M, Mokha A, Reinhorn A. Teflon bearing in base isolation II: modeling. J Struct Eng 1990;116(2):455–73.
[28] Fan FG, Ahmadi G, Tadjbakhsh IG. Multi-storey base-isolated buildings under a harmonic ground motion, Part II: sensitivity analysis. Nucl Eng Des 1990;123: 17–26.
[29] Hernried AG, Lei KM. Parametric studies on the response of equipment in resilient-friction base isolated structures subjected to ground motion. Eng Struct 1993;15:349–57.
[30] Oiles Corporation, Document No. EKS-487-02, 2008 [in Japanese].
[31] American Association of State Highway and Transportation Officials (AASHTO). AASHTO guide specifications for seismic isolation design. Washington, DC; 1991.
[32] American Association of State Highway and Transportation Officials (AASHTO). AASHTO guide specifications for seismic isolation design. Washington, DC; 1999.
[33] American Society of Civil Engineers, ASCE 7-05. Minimum design loads for buildings and other structures. ASCE standard, SEI/ASCE 7-05; 2006.
[34] CEN. Eurocode 8, design of structures for earthquake resistance—Part 1: general rules, seismic actions and rules for buildings. EN 1998-1. Comité Européen de Normalisation, Brussels; 2004.
[35] Panchal VR, Jangid RS. Variable friction pendulum system for near-fault ground motions. Struct Control Health Monit 2008;15(4):568–84.
[36] Hall JF, Heaton TH, Halling MW, Wald DJ. Near-source ground motion and its effects on flexible buildings. Earthquake Spectra 1995;11(4):569–605.
[37] Heaton TH, Hall JF, Wald DJ, Halling MV. Response of high-rise and base-isolated buildings in a hypothetical Mw 7.0 blind thrust earthquake. Science 1995;267:206–11.
[38] Jangid RS, Kelly JM. Base isolation for near-fault motions. Earthquake Eng Struct Dynam 2001;30:691–707.
[39] Gazetas G, Garini E, Anastasopoulos I, Georgarakos T. Effects of near-fault ground shaking on sliding systems. ASCE J Geotech Geoenviron Eng 2009;135(12):1906–21.
[40] Yan Xu, Lee GC. Traveling wave effect on the seismic response of a steel arch bridge subjected to near fault ground motions. Earthquake Eng Eng Vib 2007;6(3):245–57.
[41] Kalkan E, Kunnath SK. Relevance of absolute and relative energy content in seismic evaluation of structures. Adv Struct Eng 2008;11(1):1–18.
[42] Agarwal VK, Niedzwecki JM, van de Lindt JW. Earthquake induced pounding in friction varying base isolated buildings. Eng Struct 2007;29(11):2825–32.
[43] Polycarpou PC, Komodromos P. Earthquake-induced poundings of a seismically isolated building with adjacent structures. Eng Struct 2010;32: 1937–51.
[44] Yang JN, Agrawal AK. Semi-active hybrid control systems for nonlinear building against near-fault earthquakes. Eng Struct 2002;24(3):271–80.
[45] Jangid RS. Response of pure friction sliding structures to bi-directional harmonic ground motion. Eng Struct 1997;19(2):97–104.